IOP Publishing Journal of Neural Engineering
J. Neural Eng. 12 (2015) 016007 (13pp) doi:10.1088/1741-2560/12/1/016007

A comparative study of event-related coupling patterns during an auditory oddball task in schizophrenia

Alejandro Bachiller[1], Jesús Poza[1,2,3], Carlos Gómez[1], Vicente Molina[3,4], Vanessa Suazo[3] and Roberto Hornero[1,2,3]

[1] Biomedical Engineering Group, E.T.S. Ingenieros de Telecomunicación, Universidad de Valladolid, Valladolid, Spain
[2] IMUVA, Instituto de Investigación en Matemáticas, Universidad de Valladolid, Valladolid, Spain
[3] INCYL, Instituto de Neurociencias de Castilla y León, Universidad de Salamanca, Salamanca, Spain
[4] Psychiatry Department, Facultad de Medicina, Universidad de Valladolid, Valladolid, Spain

E-mail: alejandro.bachiller@uva.es

Received 8 May 2014, revised 18 September 2014
Accepted for publication 3 October 2014
Published 4 December 2014

Abstract

Objective. The aim of this research is to explore the coupling patterns of brain dynamics during an auditory oddball task in schizophrenia (SCH). *Approach.* Event-related electroencephalographic (ERP) activity was recorded from 20 SCH patients and 20 healthy controls. The coupling changes between auditory response and pre-stimulus baseline were calculated in conventional EEG frequency bands (theta, alpha, beta-1, beta-2 and gamma), using three coupling measures: coherence, phase-locking value and Euclidean distance. *Main results.* Our results showed a statistically significant increase from baseline to response in theta coupling and a statistically significant decrease in beta-2 coupling in controls. No statistically significant changes were observed in SCH patients. *Significance.* Our findings support the aberrant salience hypothesis, since SCH patients failed to change their coupling dynamics between stimulus response and baseline when performing an auditory cognitive task. This result may reflect an impaired communication among neural areas, which may be related to abnormal cognitive functions.

Keywords: neuroscience, EEG and MEG, synchronization in the nervous system, neural networks, biological signal processing

(Some figures may appear in colour only in the online journal)

1. Introduction

According to the Diagnostic and Statistical Manual of Mental Disorders, fifth edition (DSM-V) of the American Psychiatric Association (American Psychiatric Association 2013), schizophrenia (SCH) is a psychiatric disorder characterized by positive and negative symptoms, frequently accompanied by impaired cognitive processing. SCH usually starts in late adolescence or early adulthood and may become a chronic condition. It has been proposed that the longer the period of untreated psychosis, the worse the outcome (Marshall *et al* 2005). Therefore, SCH patients should be identified and treated as early as possible. It is considered a relevant socio-economic problem for health care systems. Thereby, SCH accounts for an approximately 20% decrease in life expectancy compared with the general population (Laursen *et al* 2013).

SCH has been identified as a dysconnection syndrome, which is associated with a reduced capacity to integrate information between different brain regions (Friston 1998, Stephan *et al* 2009). In addition, it has been related to an aberrant assignment of salience to external objects and internal representations (Kapur 2003). During the performance of a cognitive task, SCH patients tend to pay more

attention to non-salient events and less to salient events (Kapur 2003). Relevance attribution likely involves diverse cerebral regions and their interconnections. As a consequence, many efforts have been devoted to identifying abnormalities in the cortical connections and their relation to SCH symptoms and cognitive performance (Uhlhaas and Singer 2010).

The disconnection and aberrant salience hypotheses of schizophrenia may, at first glance, seem unrelated. However, recent formulations of the disconnection hypothesis, in terms of predictive coding and hierarchical Bayesian inference, suggest that aberrant salience can be understood in terms of aberrant precision. Precision corresponds to the salience or confidence in sensory cues and boosts sensory signals (prediction errors) that are considered to convey interesting information. Crucially, in biologically plausible predictive coding schemes, precision is encoded by the gain of neuronal populations reporting prediction errors. This means that aberrant precision corresponds to abnormalities of cortical gain control that follow from a disconnection at the synaptic level—secondary to neuromodulatory failures (Adams *et al* 2013). This is important from our perspective because one of the key determinants of gain control is synchronous activity (e.g., synchronous gain). Furthermore, the top-down control of precision or gain is thought to mediate attention that also implicates fast synchronous activity (e.g., Engel *et al* 2001, Landau, Fries 2012). In summary, we hypothesized that SCH patients would show a failure to contextualize stimulus processing through a failure to optimize the synchronous gain of neuronal populations, leading to a functional disintegration or disconnection. The physiological correlates of this disconnection would be expressed in terms of a failure to modulate synchronous activity; particularly when asked to attend to target stimuli.

Neural oscillations are the main mechanism for enabling coordinated activity during normal brain functioning. Impairments in these oscillations may contribute to pervasive network dysfunction in SCH (Uhlhaas and Singer 2010). Oscillations in low frequency ranges (delta, theta and alpha) modulate long-range synchronization (Sauseng *et al* 2004, von Stein *et al* 2000), whereas high frequency ranges (beta and gamma) reflect synchronization in both local cortical networks (Womelsdorf *et al* 2007) and large-scale networks (Uhlhaas 2013). Impaired neural oscillations in SCH may lead to functional disconnections between and within cortical regions (Friston 1998). Most SCH studies used structural magnetic resonance imaging (MRI), functional MRI or diffusion tensor imaging to study brain organization (Shenton *et al* 2001, Kubicki *et al* 2007, Gur and Gur 2010, Molina *et al* 2010). On the other hand, electroencephalography (EEG) provides high temporal resolution and allows for the assessment of the spatio-temporal patterns of neural activity and their interactions in the time range of milliseconds (Meehan and Bressler 2012, Uhlhaas 2013). In this regard, event-related potential (ERP) analyses are used to gain further insights into the neural mechanisms underlying cognitive dysfunctions (Uhlhaas *et al* 2008). ERP coupling patterns based on time-frequency representations could provide a more sensitive measure to describe SCH alterations than resting-state EEG analysis (Uhlhaas and Singer 2006, Uhlhaas 2013). In particular, SCH aberrant attribution of salience may be evidenced by task-related functional connectivity anomalies (Palaniyappan *et al* 2012a). Thereby, the examination of neural integration mechanisms may be useful for characterizing SCH pathophysiology.

In this study, all coupling parameters are measures of functional connectivity, defined as the statistical dependence between remote physiological activities. Functional neural coupling has been commonly analyzed looking at the relationships between specific sensors by means of measures of connectivity and synchrony between two signals (Varela *et al* 2001, Bruns 2004, Uhlhaas 2013). This should be contrasted with effective connectivity, which is defined as the directed or causal inference of one system over another and can be assessed by direct modification of the former (e.g., via trascranial magnetic stimulation). Our focus on various measures of functional connectivity is motivated by the notion that disconnectivity in schizophrenia is accompanied by a failure to modulate synchronous activity, which is one aspect of functional connectivity.

In this regard, ERP coherence and phase synchronization have been previously used to characterize SCH neural coupling (Ford *et al* 2002, Bob *et al* 2008). They provide an effective measure for the integration of neural ERP response (Uhlhaas 2013). In particular, transitory phase synchronization of brain activity plays an important role in neural synaptic connections (Uhlhaas *et al* 2010). Perception, memories, emotions and other complex mental processes seem to be partially supported by the transient synchronization of synaptic activity across the brain (Fell and Axmacher 2011). Nevertheless, different coupling patterns have been found depending on the applied measure (Uhlhaas 2013). Some studies reported reduced functional connections in patients, using coherence or phase synchronization, but they revealed a lack of agreement (Stephan *et al* 2009, Hinkley *et al* 2010). Several studies reported reduced functional connections in patients between frontal and temporal cortical areas (Ford *et al* 2002) and connections involving parietal and occipital cortex (Spencer *et al* 2003). Tauscher *et al* (1998) revealed a reduced local coherence for adjacent electrodes in frontal area, but they did not obtained differences for interhemispheric coherence analysis. Certainly, further studies are still required to appropriately assess neural functional connectivity patterns associated with SCH.

In order to obtain a comprehensive time-dependent characterization of neural coupling in SCH, in this study wavelet coherence (WC) and phase-locking value (PLV) have been calculated. They are useful to explore the relationship between the auditory oddball responses in different frequency bands, in terms of connectivity and synchrony. Furthermore, these connectivity and synchrony parameters have been complemented by a similarity measure: the Euclidean distance (ED). Similarity measures have been proposed to assess the statistical distance between probability distributions (Rosso *et al* 2006). Applied to brain activity, ED provides an alternative description of neural interactions. It has been

previously used to characterize neural patterns from different brain disorders, such as epilepsy (Rosso *et al* 2006), Alzheimer's disease (Bruña *et al* 2012) or cerebral ischemia (Geocadin *et al* 2000). In sum, WC, PLV and ED provide three different conceptual frameworks to study neural coupling. Hence, they will be useful to test our working hypothesis that aberrant salience in SCH is related to several deficits in processing task relevant information. On the basis of this idea, two research questions have been addressed: (i) can the proposed methodology be useful to provide further insights into the underlying brain dynamics associated with SCH?; (ii) can a global pattern of ERP coupling changes between the auditory response and pre-stimulus baseline be defined to characterize normal and SCH neural dynamics? In conclusion, we hoped to show that our complementary functional connectivity measures could disclose coupling changes induced by attended stimuli in control subjects and an attenuation of this induced functional connectivity in SCH.

2. Materials

2.1. Selection of subjects

Forty subjects were selected to participate in the study. The inclusion and exclusion criteria can be summarized as:

- Inclusion criteria: (i) total intelligence quotient (IQ) greater than 70; (ii) collaborative subjects in EEG recordings; and (iii) written informed consent obtained from patients, their caregivers and healthy volunteers.
- Exclusion criteria: (i) a case history including any neurological illness; (ii) a history of cranial trauma with loss of consciousness longer than one minute; (iii) past or present substance abuse, except nicotine or caffeine; and (iv) for the patients, presence of any other psychiatric process, and (v) for the controls, any psychiatric diagnosis present or past, or current treatment with drugs known to act on the central nervous system.

Twenty stably treated patients with paranoid SCH were included in the study. They were diagnosed according to the Diagnostic and Statistical Manual of Mental Disorders, 4th revised edition (DSM-IV-TR) criteria. The clinical status of the patients was scored using the positive and negative syndrome scale (PANSS) (Kay *et al* 1987). The Spanish version of the Wechsler adult intelligence scale, 3th edition (WAIS-III), was used to assess IQ. In addition, cognitive assessment was performed using the Spanish version of the brief assessment of cognition in SCH (BACS) scale (Segarra *et al* 2011).

Twenty age- and gender-matched healthy controls were recruited through newspaper advertisements and remunerated for their cooperation. To discard major psychiatric antecedents (personal or family background), semi-structured psychiatric interviews were previously performed.

Demographic and clinical characteristics are shown in table 1. The research boards of the University Hospitals of Valladolid and Salamanca (Spain) endorsed the study according to The Code of Ethics of the World Medical Association (Declaration of Helsinki).

Table 1. Demographic and clinical characteristics. Values are shown as 'mean ± standard deviation, SD'. NA represents 'not applicable'.

	SCH Patients	Controls
Age (years)	35.45 ± 12.07	33.35 ± 12.26
Gender (M:F)	14:6	14:6
PANSS–Positive	18.87 ± 4.39	NA
PANSS–Negative	20.93 ± 5.76	NA
PANSS–Total	74.47 ± 17.70	NA

2.2. EEG recordings

Data recording was performed using a 17-channel EEG system (BrainVision, Brain Products GmbH; Munich, Germany). Electrodes were placed in accordance with the revised international 10/20 system at Fp1, Fp2, F3, F4, F7, F8, C3, C4, P3, P4, O1, O2, T5, T6, Fz, Pz and Cz. Electrode impedance was always kept under 5 kΩ. Subjects were sat, relaxed and with their eyes closed. They were asked to stay awake and to avoid blinking. EEG recordings were performed while the participants underwent an auditory oddball task. Random series of 600 tones (whose duration was 50 ms, rise and fall time being 5 ms and intensity being 90 dB) consisted of target (500 Hz tone), distractor (1000 Hz tone) and standard (2000 Hz tone) tones with probabilities of 0.20, 0.20 and 0.60, respectively. ERP signal and stimulus markers were recorded continuously. Only attended target tones were considered in the analyses. Our focus on the attended target tones can be motivated in terms of the aberrant precision hypothesis, given that the control of precision has been linked in computational studies to attentional gain control (Adams *et al* 2013).

For each subject, 13 min of auditory response ERP activity were acquired at a sampling frequency of 250 Hz. Recordings were referenced over Cz electrode. Data were re-referenced to the average activity of all active sensors (Bledowski *et al* 2004), since common average reference is less sensitive to microssacadic artifacts in high frequency recordings (Keren *et al* 2010). Then, each ERP recording was filtered using a 50 Hz notch filter and a finite impulse response filter with a Hamming window and band-pass frequencies between 1 and 70 Hz. To minimize the presence of oculographic and myographic artifacts, a three-steps artifact rejection was carried out (Bachiller *et al* 2014). Firstly, an independent component analysis was performed to decompose ERP signals. Components related to eyeblinks were discarded according to a visual inspection of the scalp maps and their temporal activation. In a second step, continuous ERP data were segmented into 1 s-length trials ranging from −300 ms before target stimulus onset to 700 ms after onset (250 samples per trial). Finally, artifacts were automatically rejected using an adaptive thresholding method to discard ERP trials, whose amplitude exceeded a statistical-based local threshold. The numbers of selected trials for target condition

were 80.85 ± 20.62 (mean ± standard deviation, SD) and 88.75 ± 10.12 in SCH patients and controls, respectively.

3. Methods

3.1. Continuous wavelet transform

Information processing in the brain is reflected in dynamical changes of the electrical activity in time, frequency and space (Rosso *et al* 2006). Time-frequency EEG analyses provide additional information about neural synchrony, not apparent in the ongoing EEG (Roach and Mathalon 2008). In the present study, continuous wavelet transform (CWT) was used to compute the time-frequency maps. A wavelet is a zero-mean function characterized by its localization in time (Δt) and frequency (Δf) (Torrence and Compo 1998). Different waveforms can be considered to be a wavelet. In this study, the complex Morlet wavelet is used as 'mother wavelet'. It is a gaussian-windowed sinusoidal wave that provides a biologically plausible fit to the signal being modeled (Roach and Mathalon 2008). Complex Morlet wavelet is defined as follows (Mørup *et al* 2006)

$$\psi(t) = \frac{1}{\sqrt{\pi \cdot \Omega_b}} \cdot \exp\left(j2\pi\Omega_c t\right) \cdot \exp\left(\frac{-t^2}{\Omega_b}\right), \qquad (1)$$

where Ω_b is a bandwidth parameter and Ω_c is a wavelet center frequency parameter. In this analysis, both were chosen to be 1, in order to obtain a good relation between Δt and Δf at low frequencies (Hirano *et al* 2008).

A family of wavelets was formed by compressed and stretched versions of the 'mother wavelet' (Mallat 2008). The CWT of each ERP trial, $x(t)$, is defined as the convolution of $x(t)$ with a scaled and translated version of the 'mother wavelet'

$$W_x(k, s) = \frac{1}{\sqrt{s}} \cdot \int_{-\infty}^{+\infty} x(t) \cdot \psi^*\left(\frac{t-k}{s}\right) dt, \qquad (2)$$

where s represents the scaling factor, k is the time interval and * denotes the complex conjugation. The scaling factor was set to include frequencies from 1 to 70 Hz, in 0.5 Hz intervals. This approach was introduced by Tallon-Baudry *et al* (1996) and it allows to explore in detail the frequency domain.

The wavelet energy is a simple way to represent the magnitude of EEG oscillations at specific scales. Hence, the wavelet scalogram (WS) summarizes the distribution of the signal energy in the time-frequency plane (Mallat 2008). The WS is calculated as the squared modulus of the CWT coefficients

$$WS_x(k, s) = \left|W_x(k, s)\right|^2. \qquad (3)$$

On the contrary to Fourier analysis, CWT has a variable time-frequency resolution (Mallat 2008). The longest time windows were applied to the lowest frequencies, whereas the shortest time windows were applied to the highest frequencies (Roach and Mathalon 2008). A Heisenberg box was introduced by the use of the Heisenberg uncertainty principle. It is defined as a rectangle whose width depends on the time-frequency resolution, but its area remains constant (Mallat 2008). In this study, the width of the Heisenberg box was chosen to be two times the time (Δt) and frequency resolution (Δf) (Tallon-Baudry *et al* 1996). Additionally, ERP signals have an important limitation: they are finite and short-time recordings. To take this issue into account, the CWT edge effect was introduced as a variation of wavelet energy caused by a discontinuity at the edge (Torrence and Compo 1998). Hence, a cone of influence (COI) can be defined, in which edge effects can be ignored (Torrence and Compo 1998). In this study, 1 s-length target trials were decomposed into the baseline, defined as the available 300 ms pre-stimulus recording, and the response, which was evaluated in the [150 450] ms window (Bachiller *et al* 2014). Therefore, it is possible to evaluate their respective COIs by establishing the edges in the baseline [−300 0] ms and response [150 450] ms windows. Figure 1 shows two examples of scalograms where the baseline and response COI are represented.

Time-frequency analysis was evaluated in the conventional EEG frequency bands: delta (δ, 1–4 Hz), theta (θ, 4–8 Hz), alpha (α, 8–13 Hz), beta-1 (β_1, 13–19 Hz), beta-2 (β_2, 19–30 Hz) and gamma (γ, 30–70 Hz). The Heisenberg box approach was used to select the CWT coefficients corresponding to each frequency band. CWT coefficients were only considered when their associated Heisenberg boxes were completely included in the COI. Thereby, δ-band was not analyzed, since it is associated with a wavelet duration of hundreds of milliseconds. For instance, at 2 Hz this leads to a spectral bandwidth ($2 \cdot \Delta f$) of 0.64 Hz and a wavelet duration ($2 \cdot \Delta t$) of 500 ms. Hence to be correctly analyzed, a window length longer than 300 ms is needed for both response and baseline intervals.

3.2. Connectivity, synchrony and similarity measures

Brain organization cannot be fully understood if coupling between brain regions is not analyzed (Varela *et al* 2001). Functional neural coupling involves the identification of different regions that reflect a temporal correlation while subjects are performing a cognitive task (Varela *et al* 2001). Several approaches have been developed to study these neural connections. In this research, we focused on three complementary coupling measures derived from the CWT representation: (i) WC, (ii) PLV and (iii) ED.

3.2.1. Wavelet coherence (WC). Coherence has been commonly used in neuroscience to quantify the interdependencies among the neurophysiological signals measured at different electrodes (von Stein and Sarnthein 2000, Bruns 2004). ERP coherence is based on the assumption that the same patterns of physiological activity are repeated at the same latency from trial to trial (Lachaux *et al* 2002). From the CWT of two signals $x(t)$ and $y(t)$, the wavelet cross-spectrum (WCS) at time interval k and scale s

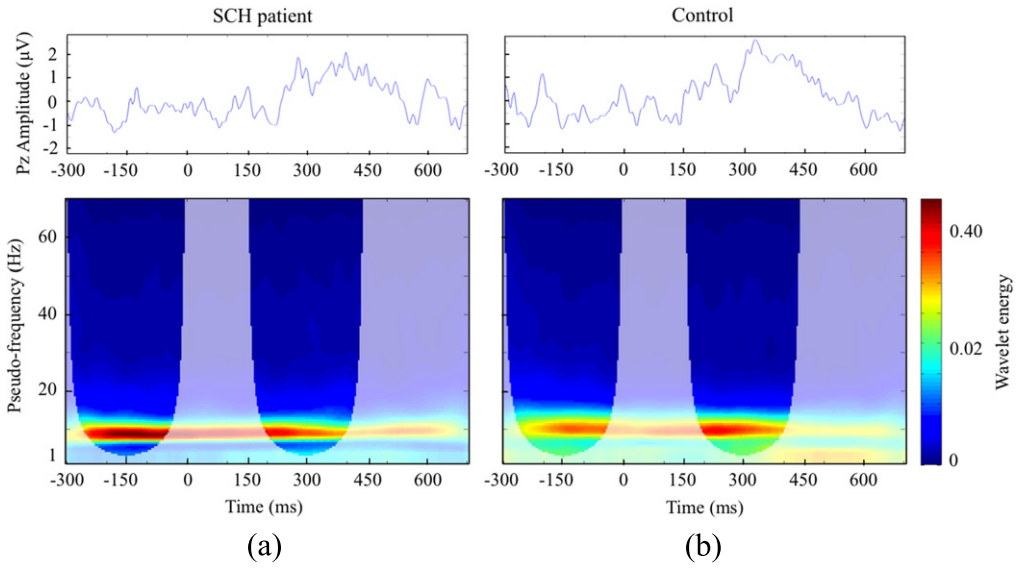

Figure 1. Averaged raw ERP and scalograms at Pz electrode for: (a) a SCH patient; (b) a healthy control. The SCH patient shows the wavelet energy concentrated in a narrow band at low frequencies. In addition, the scalogram shows a decrease of energy in the stimulus response from baseline in this band. On the other hand, the control subject shows a less concentrated wavelet energy and exhibits a slight increase of energy in the response from baseline at low frequencies. The transparency outline represents the limits of the COI, where edge effects can be ignored.

can be defined as (Lachaux *et al* 2002)

$$\mathrm{WCS}_{xy}(k, s) = \left\langle \mathrm{W}_x(k, s) \cdot \mathrm{W}_y^*(k, s) \right\rangle, \tag{4}$$

where $\langle \cdot \rangle$ denotes the average across trials.

Then, the WC between signals $x(t)$ and $y(t)$ is calculated dividing their WCS by their scalograms (Lachaux *et al* 2002)

$$\mathrm{WC}_{xy}(k, s) = \frac{\left|\mathrm{WCS}_{xy}(k, s)\right|}{\left[\mathrm{WS}_x(k, s) \cdot \mathrm{WS}_y(k, s)\right]^{1/2}}. \tag{5}$$

WC values range from 0 to 1. WC becomes 1 when the signals are perfectly coupled and 0 when they are linearly independent (Bruns 2004). Finally, a frequency-dependent WC was calculated by averaging the CWT coefficients for each frequency band

$$\mathrm{WC}_{\mathrm{band}}(k) = \left\langle \mathrm{WC}_{xy}(k, s) \right\rangle\Big|_{s\in\mathrm{band}},$$
$$\mathrm{band} = \left\{\theta, \alpha, \beta_1, \beta_2, \gamma\right\}. \tag{6}$$

3.2.2. Phase-locking value (PLV). PLV is a highly sensitive measure of neural synchronization in the EEG, useful to quantify the stability of phases between pairs of electrodes (Lachaux *et al* 1999). In contrast to WC, PLV reflects the relationship between the phases of two signals, while their amplitudes may be uncorrelated (Bob *et al* 2008). For that reason, PLV does not depend on stationarity and it is sensitive to small amplitude oscillations (Spencer *et al* 2003).

To calculate PLV, it is necessary to constrain the frequency spectrum to a narrow bandwidth and extract the instantaneous phase of every signal (Lachaux *et al* 1999). CWT approach can be used to perform filtering and phase extraction in one operation (Bob *et al* 2008). From the instantaneous phases $\varphi_x(k, s, n)$ and $\varphi_y(k, s, n)$ of two ERP signals $x(t)$ and $y(t)$, the instantaneous phase difference can be defined by

$$\Delta\varphi_{xy}(k, s, n) = \varphi_x(k, s, n) - \varphi_y(k, s, n), \tag{7}$$

where n represents each trial.

Finally, PLV evaluates the variability of the phase differences across successive trials, as follows

$$\mathrm{PLV}_{xy}(k, s) = \frac{1}{N_t}\left|\sum_{n=1}^{N_t} e^{\left(\Delta\varphi_{xy}(k,s,n)\right)}\right|, \tag{8}$$

where N_t is the total number of artifact-free trials. *PLV* is a normalized index, ranging from 0 (non-phase locked, random activity) to 1 (perfect phase synchrony) (Le Van Quyen *et al* 2001).

Analogously to WC, the PLV was calculated for each frequency band

$$\mathrm{PLV}_{\mathrm{band}}(k) = \left\langle \mathrm{PLV}_{xy}(k, s) \right\rangle\Big|_{s\in\mathrm{band}},$$
$$\mathrm{band} = \left\{\theta, \alpha, \beta_1, \beta_2, \gamma\right\}. \tag{9}$$

3.2.3. Euclidean distance (ED). Distance between statistical models is widely used in signal processing applications, such as segmentation, pattern recognition, coding or classification (Basseville 1989). The concept of distance between two probability distributions was initially developed by Mahalanobis (1936). Since then, several types of distance measures have been suggested to describe the similarity between probability distributions (Ullah 1996). In this study, we propose the use of ED to quantify the differences between the spectral content in the normalized scalogram of two different EEG electrodes. ED has been successfully applied to

characterize electromagnetic brain signals in different disorders (Rosso *et al* 2006, Bruña *et al* 2012). The normalized ED between signals $x(t)$ and $y(t)$ on each frequency band is then defined as (Ullah 1996)

$$\mathrm{ED}_{\mathrm{band}}(k) = \sum_{s\in \mathrm{band}} \left[\frac{\mathrm{WS}_{n,x}(k,\, s) - \mathrm{WS}_{n,y}(k,\, s)}{2} \right]^{1/2},$$
$$\mathrm{band} = \left\{ \theta,\, \alpha,\, \beta_1,\, \beta_2,\, \gamma \right\}, \qquad (10)$$

where $WS_{n,x}$ and $WS_{n,y}$ represent the normalized scalograms from the signals $x(t)$ and $y(t)$, respectively.

ED is a normalized dissimilarity measure, where values of 0 and 1 correspond to the highest and lowest similarity, respectively. Therefore, to obtain a direct relation with the WC and PLV, $\overline{ED} = 1 - \mathrm{ED}$ is considered.

4. Results

The coupling measures were calculated for all subjects in each frequency band, obtaining a time-frequency dependent measure from −300 ms to 700 ms. In ERP studies, it is interesting to capture event-related changes in brain activity. To this end, a baseline correction is carried out by means of the baseline [−300 0] ms and response [150 450] ms COI windows, previously defined. There are a variety of baseline-correction methods. The 'z-score approach' is commonly used, since it takes into account the variability of the baseline values (Roach and Mathalon 2008). It is noteworthy that the corrected z-values will be positive when there is a coupling increase of auditory response from baseline and they will be negative due to a coupling decrease.

In addition, two statistical analyses were performed: (i) within-groups analyses evaluate coupling changes between the baseline and the response in each frequency band by means of Wilcoxon signed-rank tests; and (ii) between-groups analyses show the differences in the pattern of coupling z-values for pathologic and control groups using Mann–Whitney U-tests.

4.1. Global analysis

As a first step, to study the global changes in EEG coupling, z-values were averaged over all electrode connections. Then, a single value per coupling parameter, band and subject was obtained. Figure 2 depicts the boxplots corresponding to the averaged z-values for each group. Afterwards, statistical analyses were performed to delimitate the frequency bands that showed statistically significant results. Initially, an exploratory analysis was used to check normality and homoscedasticity by means of the Kolmogorov-Smirnov test and Levene tests, respectively. It revealed that data did not meet parametric test assumptions. Within-groups statistical differences were evaluated by means of Wilcoxon signed-rank tests ($\alpha = 0.05$). The results are summarized in table 2; it highlights those functional connections that survived false discovery rate correction (FDR). Controls obtained a statistically significant increase of coupling between the baseline and the response in θ-band and a decrease in α, β_1 and β_2 bands. On the other hand, patients did not show statistically significant differences. These findings suggest that SCH patients were not able to change their coupling patterns when performed an oddball auditory target detection task, whereas controls exhibited significant changes in the response from the baseline.

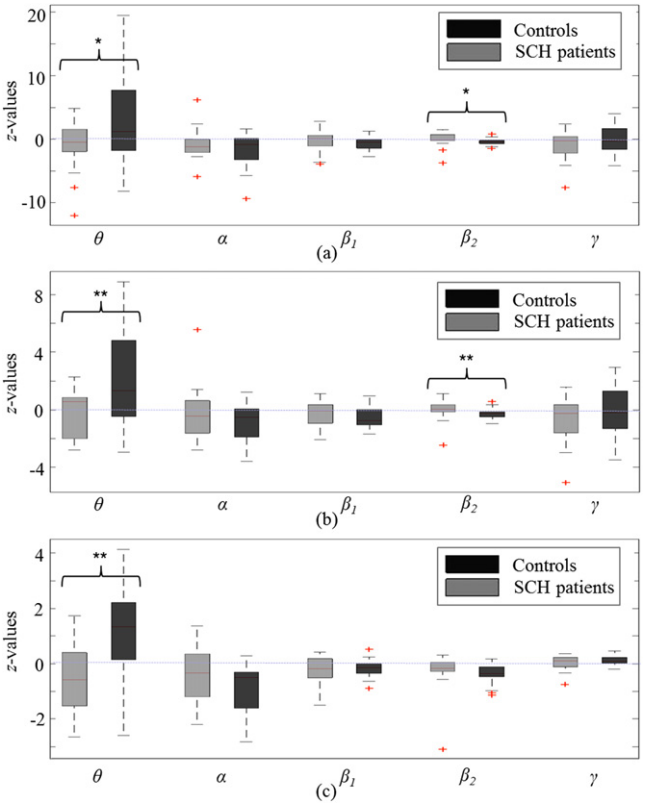

Figure 2. Boxplots displaying coupling z-values averaged over all pairs of connections at each frequency band. Positive values indicate an increase in the stimulus response compared to the baseline, whereas negative values indicate a decrease. (a) WC. (b) PLV. (c) $\overline{ED}$. Statistical analyses were performed using Mann–Whitney U-tests (*$p < 0.05$, **$p < 0.01$).

Between-groups analyses showed coupling differences between patients and controls. In detail, between-groups differences correspond to an interaction between changes in coupling and group. Mann–Whitney U-tests ($\alpha = 0.05$) were performed to assess the statistical differences. The results are summarized in table 2. Controls obtained a statistically significant increase in coupling when compared with patients in θ-band. Nevertheless, controls obtained a more statistically significant decrease than SCH patients in β_2-band.

4.2. Electrode coupling analyses

In a second step, spatial analyses were performed to explore the topographic changes in the ERP coupling patterns for the frequency bands that obtained statistically significant differences between both groups (i.e., θ and β_2). Besides, γ-band has been included since neural coupling in this band seems to play an important role to understand SCH (Uhlhaas and

Table 2. Results of Wilcoxon signed-rank tests and Mann–Whitney *U*-tests for the averaged coupling parameters. *P*-values have been FDR-corrected and statistically significant results ($p<0.05$) have been highlighted.

		Wilcoxon signed-rank test		Mann–Whitney *U*-test
Parameter	Band	SCH Patients	Controls	SCH Versus controls
WC	θ	$p>0.1$	$p=0.0402$	$p=0.0963$
	α	$p>0.1$	$p=0.0730$	$p>0.1$
	β_1	$p>0.1$	$p>0.1$	$p>0.1$
	β_2	$p>0.1$	$p=0.0467$	$p=0.0963$
	γ	$p>0.1$	$p>0.1$	$p>0.1$
PLV	θ	$p>0.1$	$p=0.0281$	$p=0.0448$
	α	$p>0.1$	$p=0.0992$	$p>0.1$
	β_1	$p>0.1$	$p=0.0289$	$p>0.1$
	β_2	$p>0.1$	$p=0.0281$	$p=0.0448$
	γ	$p>0.1$	$p>0.1$	$p>0.1$
$\overline{\text{ED}}$	θ	$p>0.1$	$p=0.0045$	$p=0.0019$
	α	$p>0.1$	$p=0.0010$	$p>0.1$
	β_1	$p>0.1$	$p=0.0187$	$p>0.1$
	β_2	$p>0.1$	$p=0.0010$	$p>0.1$
	γ	$p>0.1$	$p=0.0045$	$p>0.1$

Singer 2010). Coupling parameters were computed for all pairs of electrodes. Detailed results for coupling *z*-values between the baseline and response windows are shown in figure 3 (θ-band), figure 4 (β_2-band) and figure 5 (γ-band). Note that we did not apply a FDR correction for multiple comparisons in these topographically specific results. This is because we have already established a significant difference in terms of the average connections and report the current results as standardized effect sizes, which characterize their regional specificity. In these figures, left and central columns depict the coupling *z*-values for each group. Connections across pairs of electrodes were only displayed whether they obtained statistically significant within-groups differences between the stimulus response and the baseline (Wilcoxon signed–rank test, $|Z|>1.96$; $p<0.05$) (Fukami *et al* 2008). Statistically significant between-groups results at each frequency band are displayed in the right column of figures 3, 4 and 5. They were assessed by means of Mann–Whitney *U*-tests ($\alpha=0.05$).

Coupling analyses in θ-band show a widespread increase from baseline to response in the control group, whereas patient group exhibits a slight decrease of coupling measures, specially in frontal region (figure 3). This behavior was shown for all coupling parameters, WC, PLV and $\overline{ED}$. Within-groups analyses show that the control group obtained higher within-groups statistically significant connections than patients, mainly among electrodes on central and parietal areas. Significant differences between patients and controls are observed in the connections between frontal and central regions, central and occipital regions, central and right-temporal regions and several inter-hemispheric connections.

On the other hand, β_2-band is characterized by a decrease of coupling changes from baseline to response in both groups (figure 4). Controls show a global decrease, while SCH patients are characterized by stable coupling patterns. The distribution of *z*-values in controls reveals a significant coupling decrease from baseline to response in the connections among electrodes on frontal, central and parietal regions. Between-groups statistical analyses show significant differences, particularly between prefrontal and frontal regions, frontal and central regions, central and parietal regions and the connections between right-occipital region and several electrodes from frontal, central and parietal regions.

Despite exploratory results did not show statistically significant differences in the global analysis (figure 2 and table 2), electrode coupling analyses have provided some significant patterns for γ-band (figure 5). Patients exhibit a γ-coupling decrease from baseline to response, mainly between frontal and parietal cortical areas. On the contrary, controls show a slight increase from baseline to response in the connections with the central region. Significant differences between patients and controls are observed in the connection between electrodes in frontal and parietal regions (figure 5).

5. Discussion

The aim of this study was to characterize the neural dynamics associated with SCH. For this purpose, three coupling measures were calculated for 20 SCH patients and 20 healthy controls. Our findings suggest that SCH patients are not able to change their brain coupling as controls, when attending to target stimuli during an auditory oddball task. Therefore, neural coupling in SCH did not show statistically significant differences between the auditory stimulus response and the baseline condition. In contrast, controls exhibited several changes in the coupling patterns, specially in θ and β_2 bands.

5.1. Dynamical properties associated with SCH

The first research question pointed out in the introduction posed the issue about whether the proposed methodology provides further insights into the underlying brain dynamics associated with SCH. Most of EEG functional connectivity studies are conducted at resting-state. Nevertheless, to understand the complex relations of brain dynamics, both rest and task states should be evaluated (Turk-Browne 2013). The ERP paradigm appears then as an appropriate approach to understand how cognitive processes are performed in the brain, since it provides high temporal resolution that allows the assessment of neural events (Uhlhaas 2013, Turk-Browne 2013).

ERP data were usually analyzed using a local activation approach. Several researches focused on determining the P300 amplitude and latency, the evoked power or other spectral parameters associated with ERPs on each electrode

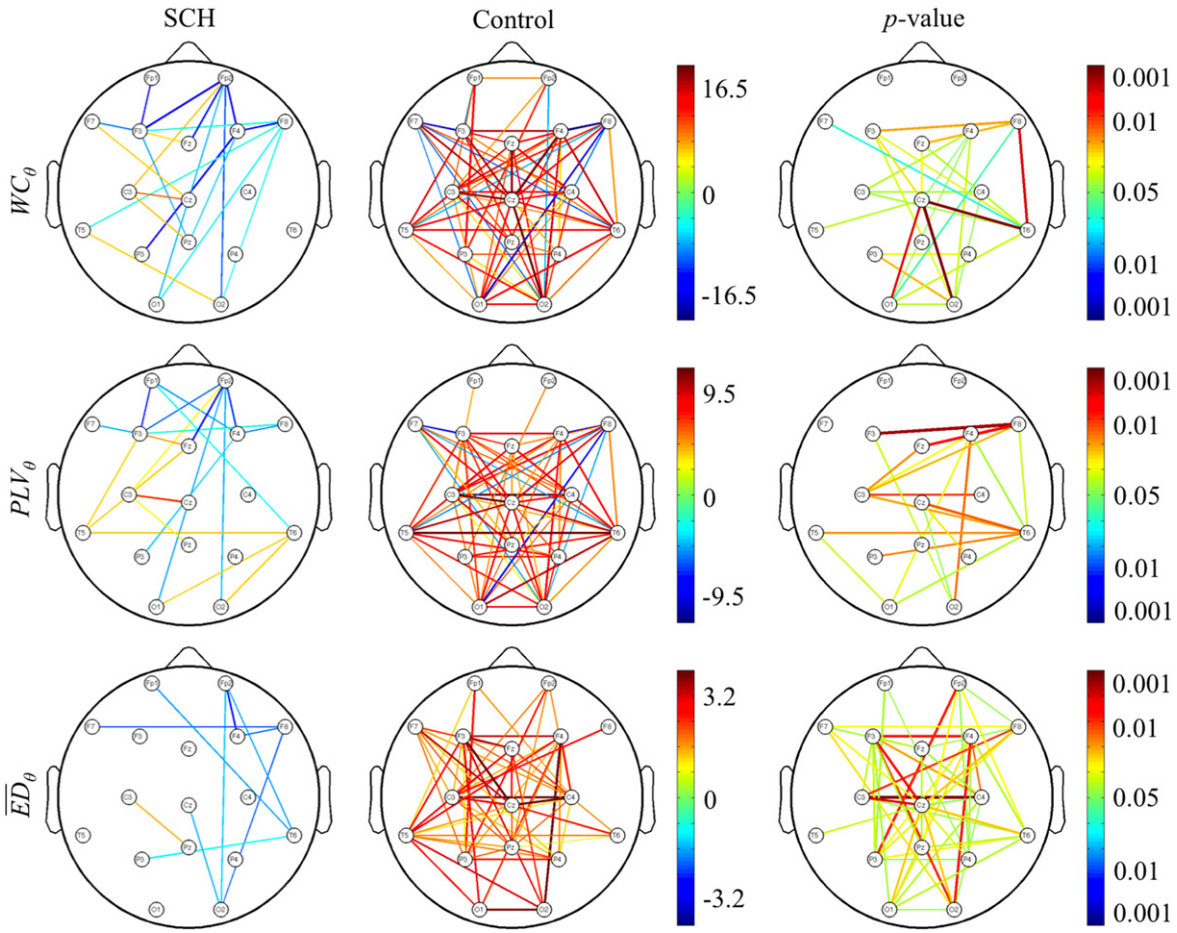

Figure 3. Spatial analyses of θ-coupling between all pairs of electrodes for WC, PLV and $\overline{ED}$. Left and central columns depict z-values for SCH patients and controls, where connections were only shown if they obtained statistically significant differences between the stimulus response and the baseline (Wilcoxon signed-rank test, $|Z|>1.96$; $p<0.05$). Right column displays statistically significant p-values between-groups (Mann–Whitney U-tests, $\alpha=0.05$). A color map was applied; in left and central columns, hot colors are associated with a coupling increase during auditory response in comparison to baseline and cold ones are assigned to a decrease. In the right column, hot colors represents smaller z-values in SCH patients than controls and cold ones higher z-values in SCH patients than controls.

(Schmiedt *et al* 2005, Roach and Mathalon 2008, Hirano *et al* 2008, Bachiller *et al* 2014). However, the study of the interactions between pairs of electrodes can provide further insights to understand the underlying neural mechanisms (Stam and Van Straaten 2012, Turk-Browne 2013). In this regard, the analysis of the amplitude and phase of neural oscillations is crucial for SCH pathophysiology characterization. The amplitude of brain oscillations has been related to the discharges of assemblies of neurons (Uhlhaas *et al* 2008), whereas phase locking has been associated with neural firing (Varela *et al* 2001). In addition, recent researches have been observed a strong correlation between phase and amplitude of neural oscillations at different frequencies (Jensen and Colgin 2007, Canolty and Knight 2010). SCH has been associated with a reduction of the amplitude from the oscillatory activity, as well as with a widespread deficit in the generation and synchronization of rhythmic activity (Uhlhaas *et al* 2008). Therefore, in order to address the underlying brain dynamics associated with SCH, we propose the analysis of ERPs neural coupling by means of three complementary measures, which consider both amplitude and phase effects.

WC and PLV have been used to assess connectivity and synchrony, respectively. Connectivity evaluates time-interdependencies between neurophysiological signals (Hinkley *et al* 2010), whereas synchrony provides an effective measure for the integration of neural responses in distributed cortical networks (Varela *et al* 2001). Thereby, they could constitute high sensitive measures for functional dysconnectivity of local and large-scale networks in SCH (Uhlhaas 2013). As showed in figures 3 and 4, connectivity and synchrony patterns are related, but these measures are not equivalent. Indeed, if two signals are synchronized, they are correlated, whereas coherence does not necessarily show the presence of synchronization (Rosemblum *et al* 2001). Connectivity and synchrony have been previously used to analyze the functional dynamics associated with SCH. Different coupling patterns were found depending on the frequency band considered. Reduced coupling from response to baseline was obtained for high frequencies, whereas a coupling increase has been showed in θ-band (von Stein and Sarnthein 2000, Ford *et al* 2002). In addition, WC and PLV were correlated with psychotic symptoms reflected by PANSS (Bob *et al* 2008).

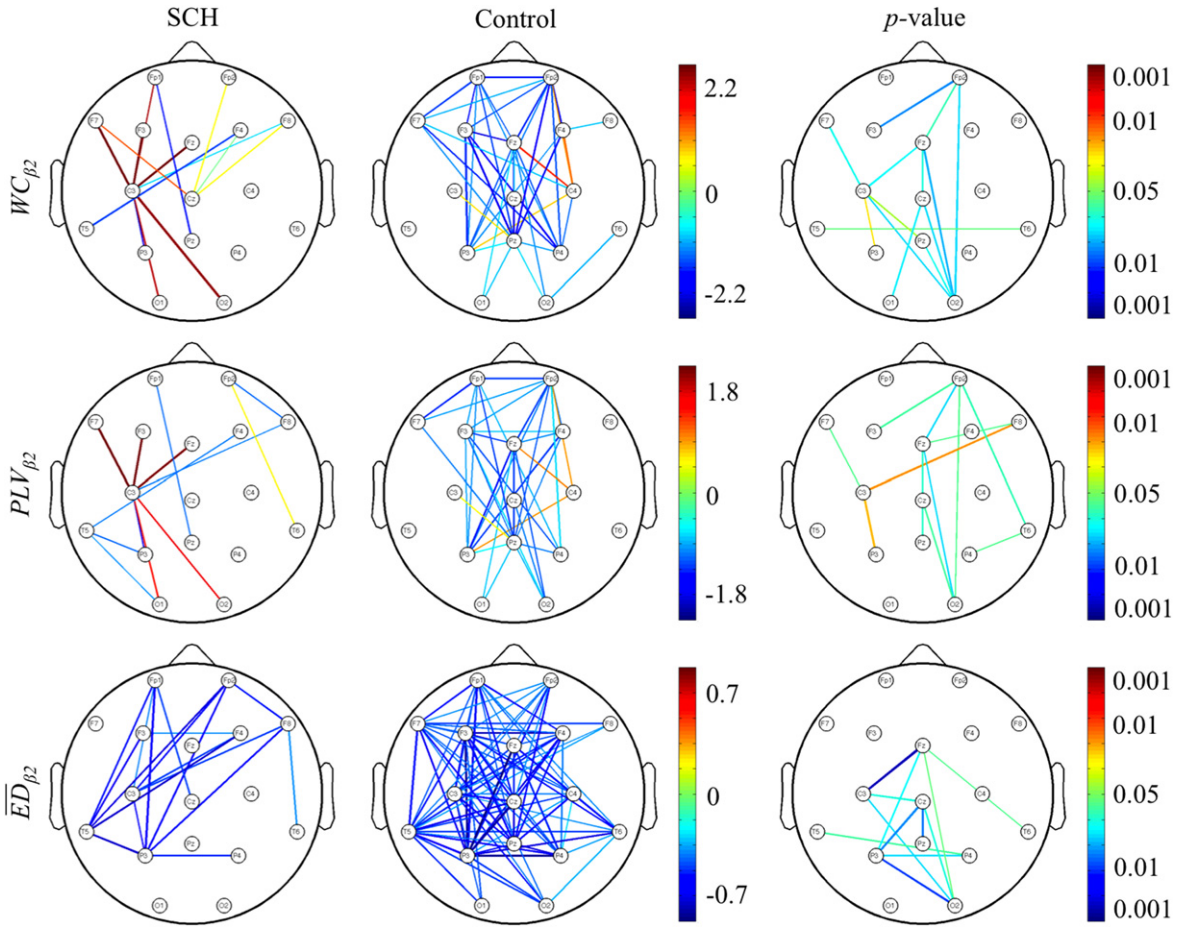

Figure 4. Spatial analyses of β_2-coupling between all pairs of electrodes for WC, PLV and $\overline{ED}$. Left and central columns depict z-values for SCH patients and controls, where connections were only shown if they obtained statistically significant differences between the stimulus response and the baseline (Wilcoxon signed-rank test, $|Z| > 1.96$; $p < 0.05$). Right column displays statistically significant p-values between groups (Mann–Whitney U-tests, $\alpha = 0.05$). A color map was applied; in left and central columns, hot colors are associated with a coupling increase during auditory response in comparison to baseline and cold ones are assigned to a decrease. In the right column, hot colors represents smaller z-values in SCH patients than controls and cold ones higher z-values in SCH patients than controls.

On the other hand, statistical distances establish a new way to explore neural coupling, introducing the concept of similarity between the spectral content of two signals in the probability space. ED and other statistical distances have been previously used as disequilibrium or irregularity measures (Rosso *et al* 2006, Bruña *et al* 2012). Nevertheless, there is a lack of studies that applied statistical distances to address the similarity between the spectral content of ERP recordings. Our results showed that similarity is better suited than connectivity and synchrony to focus on local-range interactions. As showed in figures 3 and 4, $\overline{\text{ED}}$ obtained the largest z-values and the smallest p-values for short distance links in θ and β_2 bands. On the contrary, synchrony obtained statistically significant results for large-distance links, even for several links between electrodes in different hemispheres. These results can be explained because similarity depends on the oscillations amplitude (Rosso *et al* 2006). Therefore, it may be more appropriate to measure short-distance coupling and low frequency bands.

Finally, it is noteworthy that the use of CWT can improve the understanding of neural dynamics. Wavelet analysis is better suited than Fourier and Hilbert approach for non-stationary signals, since it provides a more detailed description of the ERP time-frequency properties (Mørup *et al* 2006). Thereby, CWT approach has been proposed as a natural choice for the estimation of coupling between non-stationary signals (Lachaux *et al* 2002). In addition, using CWT, filtering and phase extraction were performed in one operation (Bob *et al* 2008), obtaining equivalent results to those obtained by means of Hilbert transform (le Van Quyen *et al* 2001).

5.2. Coupling changes pattern characterization

The second research question addressed the characterization of normal and SCH neural coupling patterns. It is well known that neural oscillations are a fundamental mechanism for enabling coordinated activity during normal brain functioning (Singer 1999). Thereby, several EEG researches support the hypothesis that distinct frequencies are involved in different computational and functional interactions (von Stein and Sarnthein 2000, Meehan and Bressler 2012, Uhlhaas 2013).

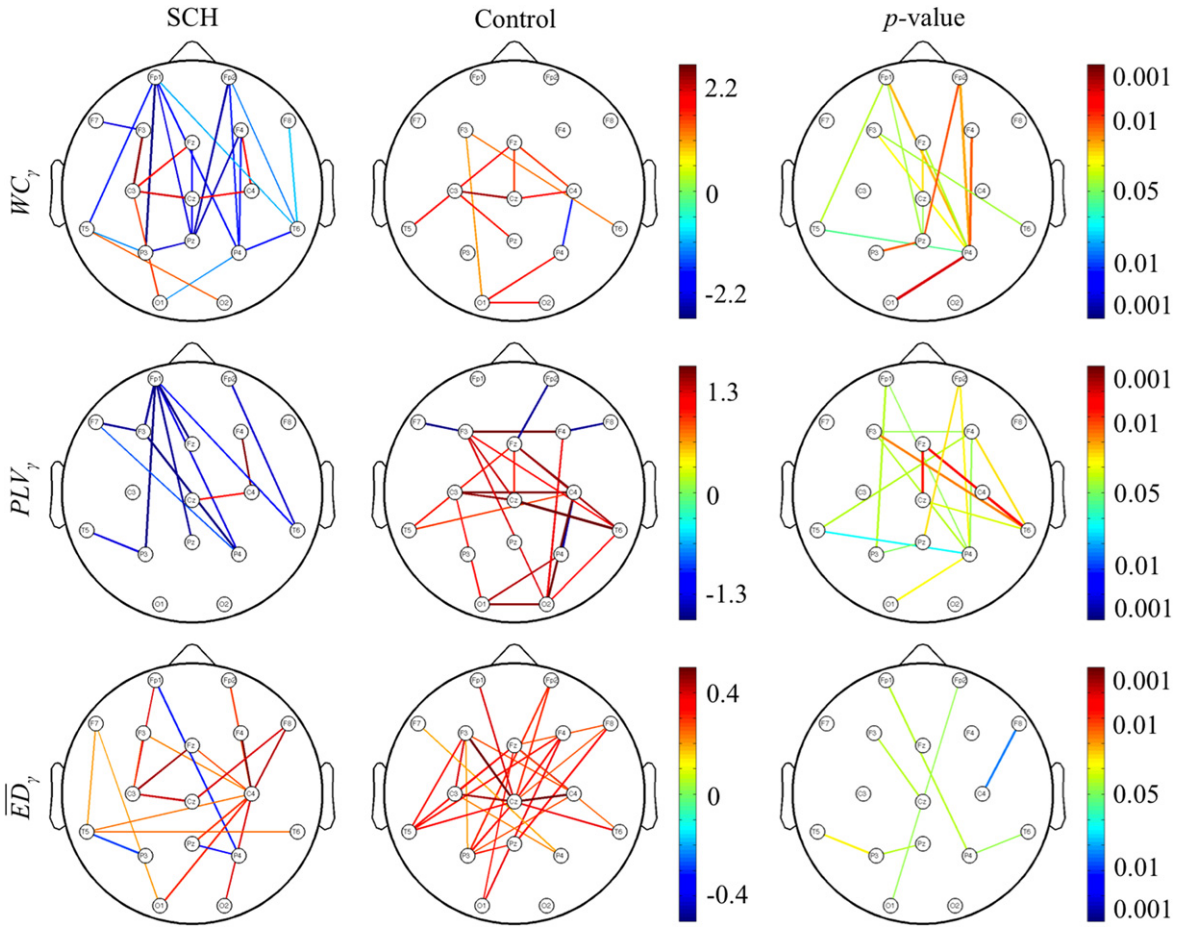

Figure 5. Spatial analyses of γ-coupling between all pairs of electrodes for WC, PLV and $\overline{ED}$. Left and central columns depict z-values for SCH patients and controls, where connections were only shown if they obtained statistically significant differences between the stimulus response and the baseline (Wilcoxon signed-rank test, $|Z| > 1.96$; $p < 0.05$). Right column displays statistically significant p-values between groups (Mann–Whitney U-tests, $\alpha = 0.05$). A color map was applied; in left and central columns, hot colors are associated with a coupling increase during auditory response in comparison to baseline and cold ones are assigned to a decrease. In the right column, hot colors represents smaller z-values in SCH patients than controls and cold ones higher z-values in SCH patients than controls.

In this research, our findings revealed the main differences in θ and β_2.

Starting with θ-band, our analyses showed a statistically significant increase of neural coupling in controls in comparison to SCH patients. The z-value differences between patients and controls are consistent with previous studies. Schmiedt *et al* (2005) obtained an increase of evoked θ-activity in controls engaged in a cognitive task, opposite to SCH patients, which did not show any change. In addition, von Stein and Sarnthein (2000) highlighted the role that θ-band neuronal synchronization plays in the interaction between frontal and posterior cortex during a cognitive task. Indeed, the deficit in θ-coupling changes in SCH patients may be related to aberrant salience hypothesis. In this regard, several researches have associated SCH with an impairment in θ-phase resetting, a gray matter reduction and a functional connectivity deficit in a defined salience network (White *et al* 2010, Palaniyappan *et al* 2012b).

In the case of β_2-band, our findings suggest that SCH patients are not able to change their coupling between the auditory response and pre-stimulus baseline. The abnormal salience in SCH may be related to a decrease neural response to relevant stimuli and to an excessive response to irrelevant tones (Kapur 2003). Thereby, SCH patients failed to respond to relevance. On the contrary, control group decreases their β_2-coupling response from baseline. Several authors suggested enhanced β_2-band synchronization in healthy controls at rest, but then it is attenuated during the cognitive response (Kilner *et al* 2000, Uhlhaas *et al* 2008). In agreement with previous studies, our findings showed several statistically significant differences in fronto-parietal connections, which have been related to cognitive tasks that involve higher executive functions (Meehan and Bressler 2012). For example, human functional MRI studies showed correlated activity between both areas in β_2-band during a cognitive task (Meehan and Bressler 2012). The analysis of coupling in beta band may be an important signature of neurocognitive network interaction. Beta-coupling is involved in long-range coordination of distributed neural activity and the synaptic connections between neurons in local cortical circuits (Uhlhaas and Singer 2010, Meehan and Bressler 2012). In this way, von Stein and Sarnthein (2000) suggested that phase

synchronization of β_2-oscillations plays a more important role than γ-synchronization on the long-distance coordination, which takes place in neurocognitive networks.

Lastly, γ-band oscillations play an important role in brain dynamics. They have been related to several brain functions, such as perception, attention, memory, consciousness and synaptic plasticity (Uhlhaas *et al* 2008). In agreement with previous studies, our findings suggest that SCH patients decrease their γ-coupling activity between response and baseline (Slewa-Younan *et al* 2004), whereas controls exhibit a γ-coupling increase (Ford *et al* 2007). Abnormal γ-band activity has also been related to disturbed corollary modulation of sensory processes (Uhlhaas *et al* 2008). Thereby, abnormal corollary discharge mechanism might be related to impaired neural γ-synchrony in patients with SCH (Uhlhaas *et al* 2008, Uhlhaas 2013). In addition, there is also a relation between abnormal γ-band and impairments in higher cognitive processes, such as executive processes and working memory (Uhlhaas *et al* 2008).

5.3. Limitations of the study and future research lines

Some limitations of this research merit consideration. Firstly, δ-band was not analyzed in this study. As we explained in 3.1 subsection, this band is influenced by edge effects due to its time resolution requirements (Torrence and Compo 1998). Thereby, future studies are needed to assess δ-coupling. Secondly, successive ERP trials have been used to compute coupling parameters. As a consequence, the induced and evoked activity has not been independently analyzed. Further work is necessary to obtain an appropriate coupling parameter that allows separating evoked and induced activity without loosing temporal resolution. Thirdly, the oscillations in cortical networks coexist in multiple frequency bands. There are several evidences that neural activity comprises interactions between oscillations at different frequencies (Le Van Quyen and Bragin 2007). Cross-frequency coupling provides a plausible mechanism for the neural coordination during perception, cognition and action functions (Canolty and Knight 2010). In particular, it has been primary observed between low and high frequency oscillations when subjects were performing different cognitive tasks (Sauseng *et al* 2008, Kirihara *et al* 2012). As a consequence, future studies should be performed to evaluate cross-frequency neural coupling. Finally, on the basis of the connections network, established by WC, PLV and ED, a complex network analysis could be addressed. We feel that it may provide very valuable insights on the structural and functional organization of neural networks in SCH.

From the perspective of predictive coding, our results are entirely consistent with the aberrant precision hypothesis of psychosis. Our data support a failure in chronic SCH patients to show an attention-dependent modulation of synchronous activity in specific frequency bands. This may reflect a failure to establish the appropriate levels of synaptic gain or precision mediating the salience of stimuli that are subsequently processed and seems coherent with a synaptic disconnection that may contribute to false inference in schizophrenia.

6. Conclusions

In summary, we found that neural coupling is altered in SCH patients during an auditory oddball task. Our results suggest that SCH patients show abnormalities in θ and β_2 bands. Specifically, controls increase their coupling between stimulus response and baseline in θ, whereas the opposite behavior is observed in β_2. On the other hand, SCH patients are not able to change their coupling dynamics, which may be related to aberrant salience in this pathology. Technically, in this research, ED was introduced for studying neural coupling patterns in terms of similarity. Our findings support the notion that ED provides original insights in comparison with the two classical connectivity and synchrony measures (WC and PLV). Further studies will address the frequency coupling between different bands and a complex network analysis.

Acknowledgements

This research was supported in part by: the 'Ministerio de Economía y Competitividad' and FEDER under project TEC2011-22987; the 'Project Cero 2011 on Ageing' from 'Fundación General CSIC, Obra Social La Caixa and CSIC'; the 'Fondo de Investigaciones Sanitarias (Instituto de Salud Carlos III)' under project FIS PI1102203; and the 'Gerencia Regional de Salud de Castilla y León' (GRS 613/A/11). A Bachiller was in receipt of a PIF-UVA grant from University of Valladolid; and V Suazo has a predoctoral scholarship from the University of Salamanca and Santander Bank.

References

Adams R A, Stephan K E, Brown H R, Frith C D and Friston K J 2013 The computational anatomy of psychosis *Front. Psychiatry* **4** 47

American Psychiatric Association 2013 *Diagnostic and Statistical Manual of Mental Disorders* 5th edn (Arlington, VA: American Psychiatric)

Bachiller A, Díez A, Suazo V, Domínguez C, Ayuso M, Hornero R, Poza J and Molina V 2014 Decreased spectral entropy modulation in patients with schizophrenia during a P300 task *Eur. Arch. Psychiatr. Clin. Neurosci.* **264** 533–43

Basseville M 1989 Distance measures for signal processing and pattern recognition *Signal Process* **18** 349–69

Bledowski C, Prvulovic D, Hoechstetter K, Scherg M, Wibral M, Goebel R and Linden D E J 2004 Localizing P300 generators in visual target and distractor processing: a combined event-related potential and functional magnetic resonance imaging study *J. Neuroscience* **24** 9353–60

Bob P, Palus M, Susta M and Glaslova K 2008 EEG phase synchronization in patients with paranoid schizophrenia *Neurosci. Lett.* **447** 73–7

Bruña R, Poza J, Gómez C, García M, Fernández A and Hornero R 2012 Analysis of spontaneous MEG activity in mild cognitive impairment and Alzheimer's disease using spectral entropies and statistical complexity measures *J. Neural Eng.* **9** 036007

Bruns A 2004 Fourier-, hilbert-and wavelet-based signal analysis: are they really different approaches? *J. Neurosci. Methods* **137** 321–32

Canolty R T and Knight R T 2010 The functional role of cross-frequency coupling *Trends Cogn. Sci.* **14** 506–15
Engel A K, Fries P and Singer W 2001 Dynamic predictions: oscillations and synchrony in top-down processing *Nat. Rev. Neurosci.* **10** 704–16
Fell J and Axmacher N 2011 The role of phase synchronization in memory processes *Nat. Rev. Neurosci.* **12** 105–18
Ford J M, Mathalon D H, Whitfield S, Faustman W O and Roth W T 2002 Reduced communication between frontal and temporal lobes during talking in schizophrenia *Biol. Psychiatry* **51** 484–92
Ford J M, Roach B J, Faustman W O and Mathalon D H 2007 Synch before you speak: auditory hallucinations in schizophrenia *Am. J. Psychiatry* **164** 458–66
Friston K J 1998 The disconnection hypothesis *Schizophr. Res.* **30** 115–25
Fukami T, Ishikawa F, Ishikawa B and Saito Y 2008 Quantitative evaluation of photic driving response for computer-aided diagnosis *J. Neural Eng.* **5** 411–21
Geocadin R G, Ghodadra R, Kimura T, Lei H, Sherman D L, Hanley D F and Thakor N V 2000 A novel quantitative EEG injury measure of global cerebral ischemia *Clin. Neurophysiol.* **111** 1779–87
Gur R E and Gur R C 2010 Functional magnetic resonance imaging in schizophrenia *Dialogues Clin. Neurosci.* **12** 333–43 http://www.dialogues-cns.org/publication/functional-magnetic-resonance-imaging-in-schizophrenia/
Hinkley L B, Owen J P, Fisher M, Findlay A M, Vinogradov S and Nagarajan S S 2010 Cognitive impairments in schizophrenia as assessed through activation and connectivity measures of magnetoencephalography (MEG) data *Front. Hum. Neurosci.* **3** 73
Hirano S *et al* 2008 Abnormal neural oscillatory activity to speech sounds in schizophrenia: a magnetoencephalography study *J. Neurosci.* **28** 4897–903
Jensen O and Colgin L L 2007 Cross-frequency coupling between neuronal oscillations *Trends Cogn. Sci.* **11** 267–9
Kapur S 2003 Psychosis as a state of aberrant salience: a framework linking biology, phenomenology, and pharmacology in schizophrenia *Am. J. Psychiatry* **160** 13–23
Kay S R, Fiszbein A and Opler L A 1987 The positive and negative syndrome scale (PANSS) for schizophrenia *Schizophr. Bull.* **13** 261–76
Keren A S, Yuval-Greenberg S and Deouell L Y 2010 Saccadic spike potentials in gamma-band EEG: characterization, detection and suppression *NeuroImage* **49** 2248–63
Kilner J M, Baker S N, Salenius S, Hari R and Lemon R N 2000 Human cortical muscle coherence is directly related to specific motor parameters *J. Neurosci.* **20** 8838–45
Kirihara K, Rissling A J, Swerdlow N R, Braff D L and Light G A 2012 Hierarchical organization of gamma and theta oscillatory dynamics in schizophrenia *Biol. Psychiat.* **71** 873–80
Kubicki M *et al* 2007 A review of diffusion tensor imaging studies in schizophrenia *J. Psychiatr. Res.* **41** 15–30
Lachaux J P, Rodriguez E, Martinerie J and Varela F J 1999 Measuring phase synchrony in brain signals *Hum. Brain Mapp.* **8** 194–208
Lachaux J P *et al* 2002 Estimating the time-course of coherence between single-trial brain signals: an introduction to wavelet coherence *Clin. Neurophysiol.* **32** 157–74
Landau A N and Fries P 2012 Attention samples stimuli rhythmically *Curr. Biol.* **22** 1000–4
Laursen T M, Nordentoft M and Mortensen P B 2013 Excess early mortality in schizophrenia *Annu. Rev. Clin. Psychol.* **10** 425–48
Le Van Quyen M *et al* 2001 Comparison of Hilbert transform and wavelet methods for the analysis of neuronal synchrony *J. Neurosci. Methods* **111** 83–98
Le Van Quyen M and Bragin A 2007 Analysis of dynamic brain oscillations: methodological advances *Trends Neurosci.* **30** 365–73
Mahalanobis P C 1936 On the generalized distance in statistics *Proc. Natl. Inst. Sci.* **2** 49–55
Mallat S 2008 *A Wavelet Tour of Signal Processing: the Sparse Way* 3rd edn (New York: Academic)
Marshall M, Lewis S, Lockwood A, Drake R, Jones P and Croudace T 2005 Association between duration of untreated psychosis and outcome in cohorts of first-episode patients: a systematic review *Arch. Gen. Psychiatry* **62** 975–83
Meehan T P and Bressler S L 2012 Neurocognitive networks: findings, models, and theory *Neurosci. Biobehav.* R **36** 2232–47
Molina V *et al* 2010 Subcortical and cortical gray matter differences between Kraepelinian and non-Kraepelinian schizophrenia patients identified using voxel-based morphometry *Psychiatry Res.* **184** 16–22
Mørup M, Hansen L K, Herrmann C S, Parnas J and Arnfred S M 2006 Parallel factor analysis as an exploratory tool for wavelet transformed event-related EEG *NeuroImage* **29** 938–47
Palaniyappan L, Doege K, Mallikarjun P, Liddle E and Francis-Liddle P 2012b Cortical thickness and oscillatory phase resetting: a proposed mechanism of salience network dysfunction in schizophrenia *Psychiatriki* **23** 117–29
Palaniyappan L, White T P and Liddle P F 2012a The concept of salience network dysfunction in schizophrenia: from neuroimaging observations to therapeutic opportunities *Curr. Top. Med. Chem.* **12** 2324–38
Roach B J and Mathalon D H 2008 Event-related EEG time-frequency analysis: an overview of measures and an analysis of early gamma band phase locking in schizophrenia *Schizophr. Bull.* **34** 907–26
Rosenblum M, Pikovsky A, Kurths J, Schäfer C and Tass P A 2001 Phase synchronization: from theory to data analysis *Handbook Biol. Phys.* **4** 279–321
Rosso O A, Martin M T, Figliola A, Keller K and Plastino A 2006 EEG analysis using wavelet-based information tools *J. Neurosci. Methods* **153** 163–82
Sauseng P, Klimesch W, Doppelmayr M, Hanslmayr S, Schabus M and Gruber W R 2004 Theta coupling in the human electroencephalogram during a working memory task *Neurosci. Lett.* **354** 123–6
Sauseng P, Klimesch W, Gruber W R and Birbaumer N 2008 Cross-frequency phase synchronization: a brain mechanism of memory matching and attention *Neuro. Image* **40** 308–17
Schmiedt C, Brand A, Hildebrandt H and Basar-Eroglu C 2005 Event-related theta oscillations during working memory tasks in patients with schizophrenia and healthy controls *Cogn. Brain Res.* **25** 936–47
Segarra N *et al* 2011 Spanish validation of the brief assessment in cognition in schizophrenia (BACS) in patients with schizophrenia and healthy controls *Eur. Psychiatry* **26** 69–79
Shenton M E, Dickey C C, Frumin M and McCarley R W 2001 A review of MRI findings in schizophrenia *Schizophr. Res.* **49** 1–52
Singer W 1999 Neuronal synchrony: a versatile code for the definition of relations? *Neuron* **24** 49–65
Slewa-Younan S *et al* 2004 Sex differences in functional connectivity in first-episode and chronic schizophrenia patients *Am. J. Psychiatry* **161** 1595–602
Spencer K M, Nestor P G, Niznikiewicz M A, Salisbury D F, Shenton M E and McCarley R W 2003 Abnormal neural synchrony in schizophrenia *J. Neurosci.* **23** 7407–11 (www.jneurosci.org/content/23/19/7407.full)
Stam C J and Van Straaten E C W 2012 The organization of physiological brain networks *Clin. Neurophysiol.* **123** 1067–87

Stephan K E, Friston K J and Frith C D 2009 Dysconnection in schizophrenia: from abnormal synaptic plasticity to failures of self-monitoring *Schizophr. Bull.* **35** 509–27

Tallon-Baudry C, Bertrand O, Delpuech C and Pernier J 1996 Stimulus specificity of phase-locked and non-phase-locked 40 Hz visual responses in human *J. Neurosci.* **16** 4240–9 (www.jneurosci.org/content/16/13/4240.short)

Tauscher J, Fischer P, Neumeister A, Rappelsberger P and Kasper S 1998 Low frontal electroencephalographic coherence in neuroleptic-free schizophrenic patients *Biol. Psychiatry* **44** 438–47

Torrence C and Compo G P 1998 A practical guide to wavelet analysis *Bull. Am. Meteorol. Soc.* **79** 61–78

Turk-Browne N B 2013 Functional interactions as big data in the human brain *Science* **342** 580

Uhlhaas P J, Haenschel C, Nikolić D and Singer W 2008 The role of oscillations and synchrony in cortical networks and their putative relevance for the pathophysiology of schizophrenia *Schizophrenia Bull.* **34** 927–43

Uhlhaas P J and Singer W 2006 Neural synchrony in brain disorders: relevance for cognitive dysfunctions and pathophysiology *Neuron* **52** 155–68

Uhlhaas P J, Roux F, Rodriguez E, Rotarska-Jagiela A and Singer W 2010 Neural synchrony and the development of cortical networks *Trends Cogn. Sci.* **14** 72–80

Uhlhaas P J and Singer W 2010 Abnormal neural oscillations and synchrony in schizophrenia *Nat. Rev. Neurosci.* **11** 100–13

Uhlhaas P J 2013 Dysconnectivity, large-scale networks and neuronal dynamics in schizophrenia *Curr. Opin. Neurobiol.* **23** 283–90

Ullah A 1996 Entropy, divergence and distance measures with econometric applications *J. Stat. Plan. Infer.* **49** 137–62

Varela F, Lachaux J P, Rodriguez E and Martinerie J 2001 The brainweb: phase synchronization and large-scale integration *Nat. Rev. Neurosci.* **2** 229–39

von Stein A, Chiang C and König P 2000 Top-down processing mediated by interareal synchronization *Proc. Natl. Acad. Sci. USA* **97** 14748–53

von Stein A and Sarnthein J 2000 Different frequencies for different scales of cortical integration: from local gamma to long range alpha/theta synchronization *Int. J. Psychophysiol.* **38** 301–13

White T P, Joseph V, Francis S T and Liddle P F 2010 Aberrant salience network (bilateral insula and anterior cingulate cortex) connectivity during information processing in schizophrenia *Schizophr. Res.* **123** 105–15

Womelsdorf T, Schoffelen J M, Oostenveld R, Singer W, Desimone R, Engel A K and Fries P 2007 Modulation of neuronal interactions through neuronal synchronization *Science* **316** 1609–12